Journal of Ovarian Research

RESEARCH Open Access

Sempervirine inhibits proliferation, invasion and metastasis of ovarian cancer cells and induces ultrastructural changes in vivo

Danni Chen[1,2†], Yan Tan[2†], Tingting Chen[2†], Qin Wang[2], Yan Yan[2], Xiaoya Zhao[1,3*], Zhongxiao Zhang[2*], Jin Qiu[2*] and Jian Zhang[1,3*]

Abstract

Ovarian cancer is one of the deadliest gynecological malignancies due to its late diagnosis and easy recurrence. Therefore, it is urgent to develop novel therapeutics for ovarian cancer treatment. In this study, we evaluated the anti-ovarian cancer effects of sempervirine in vitro and in vivo. CCK8 assays showed that sempervirine dose-dependently inhibited the proliferation of SKOV3 ovarian cancer cells. Transwell assays demonstrated that sempervirine significantly suppressed the invasion and metastasis of SKOV3 cells. Furthermore, in an orthotopic ovarian cancer mouse model, sempervirine dramatically inhibited tumor growth and induced pathological changes in tumor tissues, including poor development of tumor mucosa, collagen deposition, endoplasmic reticulum damage, mitochondrial swelling and vacuolar degeneration, which were similar to the positive control 5-Fu. Mechanistic studies revealed that sempervirine decreased the expression of proteins related to apelin signaling pathway. In conclusion, our results demonstrate the potent anti-ovarian cancer effects of sempervirine both in vitro and in vivo. Sempervirine may repress ovarian cancer by down-regulating apelin signaling pathway. Our study suggests that sempervirine is a promising therapeutic agent against ovarian cancer.

Introduction

Ovarian cancer is one of the three major malignant tumors of the female reproductive system and the leading cause of death from gynecological cancers worldwide [1, 2]. The overall 5-year survival rate of ovarian cancer patients is less than 50% [3]. The high mortality rate is largely attributed to the asymptomatic nature of early-stage disease, resulting in about 75% of patients being diagnosed at an advanced stage (stage III or IV) [4]. For advanced ovarian cancer, the standard treatment is aggressive cytoreductive surgery followed by platinum-based chemotherapy [5]. Although most patients initially respond well to chemotherapy and attain clinical remission, recurrence occurs in over 70% of cases [6]. Recurrent ovarian cancer is resistant to further platinum therapy and ultimately progresses to death [7]. Moreover,

†Danni Chen, Yan Tan and Tingting Chen contributed equally to this work.

*Correspondence:
Xiaoya Zhao
zxyyy618@163.com
Zhongxiao Zhang
zhangzhongxio2005@163.com
Jin Qiu
QJ4098@shtrhospital.com
Jian Zhang
zhangjian_ipmch@sjtu.edu.cn
[1]Department of Obstetrics and Gynecology, The International Peace Maternity and Child Health Hospital, School of Medicine, Shanghai Jiao Tong University, Shanghai 200030, China
[2]Department of Obstetrics and Gynecology, Tongren Hospital, Shanghai Jiao Tong University School of Medicine, Shanghai 200336, China
[3]Shanghai Key Laboratory of Embryo Original Diseases, Shanghai 200030, China

current chemotherapeutic drugs have many adverse effects that impact the quality of life of patients [8]. Therefore, it is imperative to identify novel agents and develop more effective therapies with lower side effects for ovarian cancer.

Natural products have been valuable sources for anticancer drug discovery over the past decades [9]. More than 60% of anticancer drugs are derived directly or indirectly from natural sources, such as plants, marine organisms and microorganisms [10]. Plant-derived compounds in particular have made great contributions to cancer chemotherapy. Well-known examples include paclitaxel and camptothecin, which are isolated from Pacific yew tree and Camptotheca acuminata, respectively [11]. Phytochemical studies have identified various alkaloids from Bulbus Fritillaria as the main bioactive components with anticancer properties [12].

Sempervirine is a bioactive alkaloid isolated from the traditional Chinese medicinal plant Gelsemium elegans Benth. (Loganiaceae) [13]. While G. elegans extracts have been used historically for treating skin ulcers, headaches, and cancer, the clinical use has been limited due to toxicity [14]. Sempervirine was first isolated from G. elegans in 1949 and its structure characterized [15]. Recent studies have synthesized sempervirine derivatives and elucidated structure-activity relationships [16–18]. Sempervirine exhibits cytotoxicity against several cancer cell lines including breast, cervical, lymphoma, and testicular cancers by inhibiting RNA polymerase I transcription in a p53-independent manner [16, 19, 20]. Of note, sempervirine appears to selectively target cancer cells over normal cells by binding to RPA194 [20]. The selective anticancer cytotoxicity and potential to cross the blood-brain barrier due to its low molecular weight make sempervirine a promising candidate for further development as a novel chemotherapeutic agent, including for intracranial tumors. The anticancer mechanisms of sempervirine involve inducing cell cycle arrest, apoptosis, autophagy, and inhibition of Wnt/β-catenin signaling [21]. Recent studies also found that sempervirine could enhance the sensitivity of breast and ovarian cancer cells to chemotherapeutic drugs [22]. However, the effects of sempervirine on ovarian cancer and the underlying mechanisms remain unclear.

In this study, we evaluated for the first time the in vitro and in vivo anti-ovarian cancer effects of sempervirine using the human ovarian cancer cell line SKOV3 and an orthotopic ovarian cancer mouse model. We found that sempervirine significantly inhibited ovarian cancer cell proliferation, invasion, metastasis and tumor growth. Sempervirine also induced ultrastructural changes in ovarian tumor tissues similar to the first-line chemotherapy drug 5-fluorouracil. Mechanistic studies showed that the anticancer effects of sempervirine are mediated through downregulation of the apelin signaling pathway. Our results provide strong experimental evidence supporting the development of sempervirine as a promising therapeutic agent for ovarian cancer treatment.

Materials and methods

Cell lines and cell culture

Human ovarian cancer cell lines SKOV3 was purchased from the Type Culture Collection of the Chinese Academy of Sciences (Shanghai, China). Cells were cultured in RPMI 1640 medium supplemented with 10% fetal bovine serum (FBS), 100 U/ml penicillin, and 100 μg/ml streptomycin. Cells were maintained at 37 °C in a humidified atmosphere containing 5% CO2.

Reagents and antibodies

Sempervirine (purity ≥ 98%) was obtained from Yuanye Biotechnology (Shanghai, China). 5-Fluorouracil (5-Fu) was purchased from Sigma-Aldrich. Primary antibodies against apelin, CD34 and GAPDH were purchased from Cell Signaling Technology. Horseradish peroxidase (HRP)-conjugated secondary antibodies were obtained from Santa Cruz Biotechnology.

Cell proliferation assay

The effect of sempervirine on ovarian cancer cell proliferation was determined by CCK8 assay. SKOV3 cells were seeded into 96-well plates at a density of 5 × 103 cells/well and cultured overnight. Cells were then treated with various concentrations of sempervirine (0, 0.1, 0.5, 1, 5, 10, 25, 50, 100 μM) for 6 h, 24 h and 48 h. CCK8 solution (Beyotime Institute of Biotechnology) was added to each well followed by 2 h incubation at 37 °C. The absorbance at 450 nm was measured using a microplate reader (Bio-Rad). Cell viability was calculated as the percentage of control cells without drug treatment.

Transwell invasion assays

The effects of sempervirine on ovarian cancer cell invasion were evaluated using transwell chambers (8 μm pore size, Corning). For invasion assay, the upper chamber was precoated with Matrigel (BD Biosciences). SKOV3 cells were pretreated with sempervirine (0, 1, 5, 10 μM) for 24 h, resuspended in serum-free medium and then seeded into the upper chambers at a density of 5 × 104 cells/chamber. The lower chambers were filled with medium containing 10% FBS as chemoattractant. After 24 h incubation, the non-migrating or non-invading cells on the upper surface were removed gently with a cotton swab. The cells on the lower surface were fixed with 4% paraformaldehyde, stained with 0.1% crystal violet and photographed under a microscope. Five random fields were captured and the number of migrated or invaded cells was counted.

Colony formation assay

The effect of sempervirine on SKOV3 cell proliferation was assessed using a colony formation assay. Cells were trypsinized and seeded at a density of 500 cells per well in 6-well plates. Following a 24-hour incubation, cells were treated with different concentrations of sempervirine (2.5 μM, 5 μM, 10 μM) or with vehicle (control group) for 48 h. After treatment, the drug-containing medium was replaced with drug-free medium, and the cells were cultured for an additional 7 days, with the medium being refreshed every 2 days. After 7 days, cells were fixed with 4% paraformaldehyde for 30 min at room temperature, followed by staining with 0.1% crystal violet for 30 min. Stained plates were washed with sterile water and allowed to dry, and colonies were counted manually.

Apoptosis analysis by flow cytometry

Apoptosis induction by sempervirine was assessed using an Annexin V-APC/PI double staining method. SKOV3 cells were seeded at a density of 1.5×10^5 cells per well in 6-well plates. After adherence, cells were treated with sempervirine at various concentrations (2.5 μM, 5 μM, 10 μM) for 24 h. Cells were then harvested using trypsin without EDTA, washed twice with PBS, and resuspended in 500 μL of Binding Buffer. Next, 5 μL of Annexin V-APC and 5 μL of PI staining solution were added to the cell suspension, followed by gentle mixing. The cells were incubated at room temperature for 5–10 min in the dark. Apoptosis was analyzed within 1 h using flow cytometry (BD Biosciences) with excitation at 633 nm and emission detection at 660 nm. Fluorescence compensation was performed using apoptosis-induced cells as a control.

Cell cycle analysis

To investigate the effect of sempervirine on the cell cycle, SKOV3 cells were seeded at a density of 1.5×10^5 cells per well in 6-well plates and treated with sempervirine at 2.5 μM, 5 μM, and 10 μM concentrations for 24 h. Cells were then harvested by trypsinization, washed twice with PBS, and fixed with 70% pre-chilled ethanol overnight at 4 °C. Fixed cells were centrifuged at 500 g for 5 min, the supernatant was discarded, and cells were washed with pre-chilled PBS three times. Cells were resuspended in propidium iodide (PI) staining solution and incubated at room temperature for 30 min. Cell cycle distribution was analyzed by flow cytometry, and the proportions of cells in the G0/G1, S, and G2/M phases were determined.

RNA extraction, library preparation and sequencing

Total RNAs were extracted from SKOV3 cells using TRIzol Reagent (Invitrogen, cat. NO 15596026)following the protocol. Post-extraction, genomic DNA contamination was removed by treatment with DNase I. RNA quality and purity were assessed by measuring the A260/A280 ratio using a NanoDrop™ OneC spectrophotometer (Thermo Fisher Scientific). RNA integrity was further confirmed through 1.5% agarose gel electrophoresis, and RNA concentration was accurately quantified using the Qubit™ RNA Broad Range Assay Kit (Life Technologies, Cat. No. Q10210) on a Qubit 3.0 fluorometer.

For stranded RNA sequencing library preparation, 2 μg of total RNA was processed using the KC-Digital™ Stranded mRNA Library Prep Kit for Illumina® (Cat. No. DR08502, Wuhan Seqhealth Co., Ltd., China) according to the manufacturer's instructions. This kit minimizes PCR and sequencing duplication bias by incorporating an 8-base unique molecular identifier (UMI) to label pre-amplified cDNA molecules. Library fragments between 200 and 500 bp were enriched, quantified, and subsequently sequenced using the DNBSEQ-T7 sequencer (MGI Tech Co., Ltd., China) with paired-end 150 bp reads.

RNA-Seq data analysis

Raw sequencing data were first processed using Trimmomatic (version 0.36) to remove low-quality reads and trim adaptor sequences. Clean reads were further refined using custom scripts to eliminate duplication bias introduced during library preparation and sequencing. Specifically, clean reads were clustered based on unique molecular identifiers (UMIs), grouping reads with identical UMI sequences into the same cluster. Pairwise alignment was then performed within each cluster, and reads with greater than 95% sequence identity were grouped into sub-clusters. For each sub-cluster, multiple sequence alignment was used to generate a single consensus sequence, effectively correcting for errors and biases from PCR amplification and sequencing. These deduplicated consensus sequences were used for downstream RNA-seq analysis.

Subsequently, the deduplicated reads were mapped to the human reference genome using STAR (version 2.5.3a) with default parameters. Reads aligned to the exon regions of each gene were quantified using feature Counts (Subread-1.5.1, Bioconductor), and gene expression levels were calculated as reads per kilobase of transcript per million mapped reads (RPKM). Differentially expressed genes between experimental groups were identified using the edgeR package (version 3.12.1), with a p-value cutoff of 0.05 and a fold-change threshold of 2 considered statistically significant.

Gene Ontology (GO) analysis and Kyoto Encyclopedia of Genes and Genomes (KEGG) enrichment analysis for differentially expressed genes were conducted using KOBAS software (version 2.1.1), with a p-value threshold of 0.05 indicating significant enrichment. Alternative splicing events were identified using rMATS (version

3.2.5), with a false discovery rate (FDR) cutoff of 0.05 and an absolute Δψ threshold of 0.05.

Western blot analysis

Total protein was extracted from ovarian cancer cells using RIPA lysis buffer containing protease and phosphatase inhibitors. The protein concentration was determined by BCA assay. Equal amounts of protein samples were separated by 10% SDS-PAGE and transferred onto PVDF membranes. The membranes were blocked in 5% non-fat milk for 1 h and incubated with primary antibodies at 4 °C overnight, followed by incubation with HRP-conjugated secondary antibodies for 1 h at room temperature. Protein bands were visualized using ECL reagents and band intensity was quantified by ImageJ software.

In vivo xenograft model

All animal experiments were approved by the Institutional Animal Care and Use Committee of shanghai tongren hospital. Female BALB/c nude mice (5–6 weeks old) were purchased from Vital River Laboratory (Beijing, China). SKOV3 cells (2 × 106) in 100 μLPBS were subcutaneously injected into the right flank of each mouse to establish the ovarian cancer xenograft model. When the tumor volume reached about 100 mm [3], the mice were randomized into three groups ($n = 6$ per group) and treated as follows: (1) Control group: 100 μL normal saline by intraperitoneal injection every two days; (2) 5-Fu group: 5-Fu at 1 mg/kg by intraperitoneal injection every two days; (3) Sempervirine group: sempervirine at low-dose1mg/kg; mediun-dose 3 mg/kg, high-dose10 mg/kg by intraperitoneal injection every two days. After 15 days treatment, mice were sacrificed and tumors were excised and weighed. Tumor tissues were collected for further analysis.

Immunohistochemistry (IHC)

Tumor tissues were fixed, embedded in paraffin and sectioned at 5 μm thickness. The sections were deparaffinized, rehydrated and subjected to antigen retrieval. After blocking with bovine serum albumin (BSA), the slides were incubated with Ki-67 primary antibody overnight at 4 °C, followed by incubation with biotinylated secondary antibody and HRP-conjugated streptavidin. The signaling was developed using DAB solution and counterstained with hematoxylin.

Statistical analysis

All experiments were performed in triplicate. Data were expressed as mean ± standard deviation. Statistical analysis was performed using GraphPad Prism 7 software. Differences between groups were analyzed by one-way ANOVA or Student's t-test. $p < 0.05$ was considered statistically significant.

Results

Sempervirine inhibits ovarian cancer cell proliferation in vitro

To investigate the effects of sempervirine on ovarian cancer cell proliferation, SKOV3 human ovarian cancer cells were treated with increasing concentrations of sempervirine for 6, 12 and 24 h. Cell viability was determined by CCK8 assays. As shown in Fig. 1A and B, sempervirine significantly reduced the proliferation of SKOV3 cells in a dose- and time-dependent manner. These results demonstrate the potent antiproliferative effects of sempervirine against ovarian cancer cells in vitro.

Sempervirine inhibits the invasion of ovarian cancer cells

Sempervirine is a bioactive alkaloid derived from traditional Chinese herbs. As shown in Figure S1., sempervirine contains a four-ring steroid core structure with an

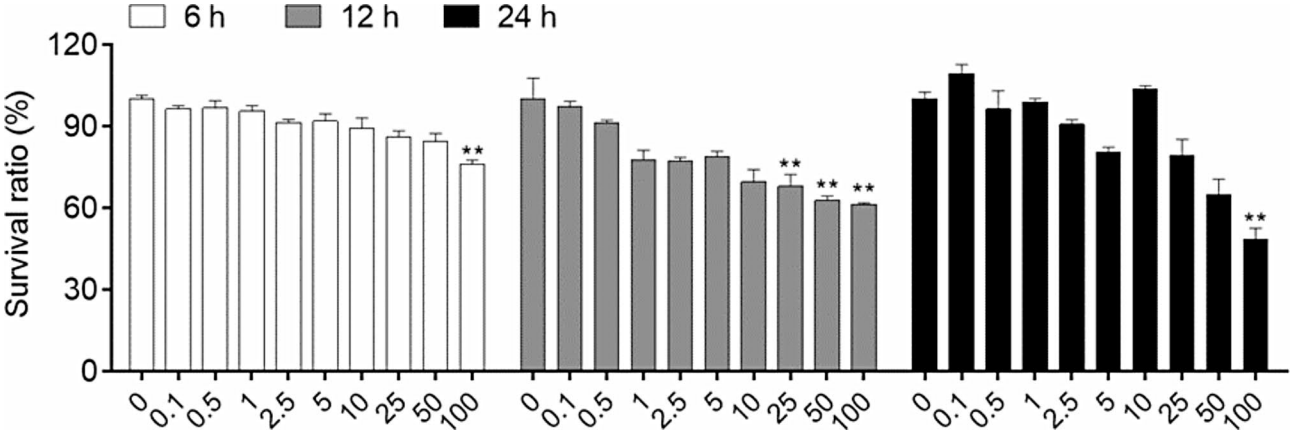

Fig. 1 Sempervirine inhibits proliferation of ovarian cancer cells in a dose-dependent manner.Ovarian cancer SKOV3 cells were treated with various concentrations of sempervirine (0.1μM, 0.5μM, 1μM, 5μM, 10μM, 50μM, 100μM) for 6 h,12 h and 24 h. Cell proliferation was measured using CCK8 assays. Data are presented as mean ± SD of three independent experiments. *$P < 0.05$, **$P < 0.01$, ***$P < 0.001$ vs. 0 μM control

isoquinoline group. We examined the effects of sempervirine on ovarian cancer cell invasion using SKOV3 cells. Cells were treated with varying concentrations of sempervirine for 24 h prior to assessment of invasion through transwell inserts.Sempervirine significantly inhibited SKOV3 cell invasion in a dose-dependent manner. At 1μM,10μM concentration, sempervirine nearly abolished cell invasion. These data indicate sempervirine's potential as an anti-metastatic agent against ovarian cancer cells by suppressing cell invasion. Further studies are warranted to elucidate the molecular mechanisms.

Sempervirine induces ultrastructural changes in ovarian tumor tissues

We further validated the antitumor efficacy of sempervirine in vivo using a subcutaneous SKOV3 xenograft mouse model. Transmission electron microscopy was utilized to evaluate the effects of sempervirine on the ultrastructure of ovarian tumor tissues. As presented in Figure.S2, control tumors displayed normal cell morphology with intact membranes, evenly dispersed chromatin and well-developed organelles. In contrast, sempervirine-treated tumors exhibited shrunken nuclei with condensed chromatin, swollen mitochondria, disrupted endoplasmic reticulum, increased cytoplasmic vacuoles and blurred cell boundaries, indicative of tumor cell damage. These ultrastructural alterations were comparable to the positive control 5-Fu. Thus, sempervirine could induce tumor cell ultrastructural changes in vivo.

Sempervirine exhibits potent antitumor efficacy in orthotopic ovarian cancer model

The pathological changes of tumor tissues from different mouse groups were compared. Hematoxylin and eosin (H&E) staining showed that poorly developed tumor mucosa was significantly increased in the treatment group compared to the control group. The results indicate that the compound successfully induced histopathological alterations of tumors. Samples from tumors of each group were obtained for transmission electron microscopy analysis. As shown in the figure, compared to the control group, irregular morphologies including collagen deposition, endoplasmic reticulum damage, mitochondrial swelling, and vacuolar degeneration were observed in the treatment group. Notably, the ultrastructural improvements by the high-dose compound were comparable to that of the positive control 5-Fu group.

As shown in Fig. 2, tumor sections from control mice exhibited typical histological architecture and tissue organization. In contrast, tumors from sempervirine-treated mice showed regions of poor mucosal development, indicating disruption of normal tumor structure. These results demonstrate that sempervirine can effectively induce pathological changes and architectural damage in tumor tissues in vivo. The induction of abnormal tissue morphology provides evidence that sempervirine may inhibit tumor growth through detrimental effects on tumor integrity and developmental processes. Further investigation of the molecular basis of sempervirine's anticancer effects is warranted.

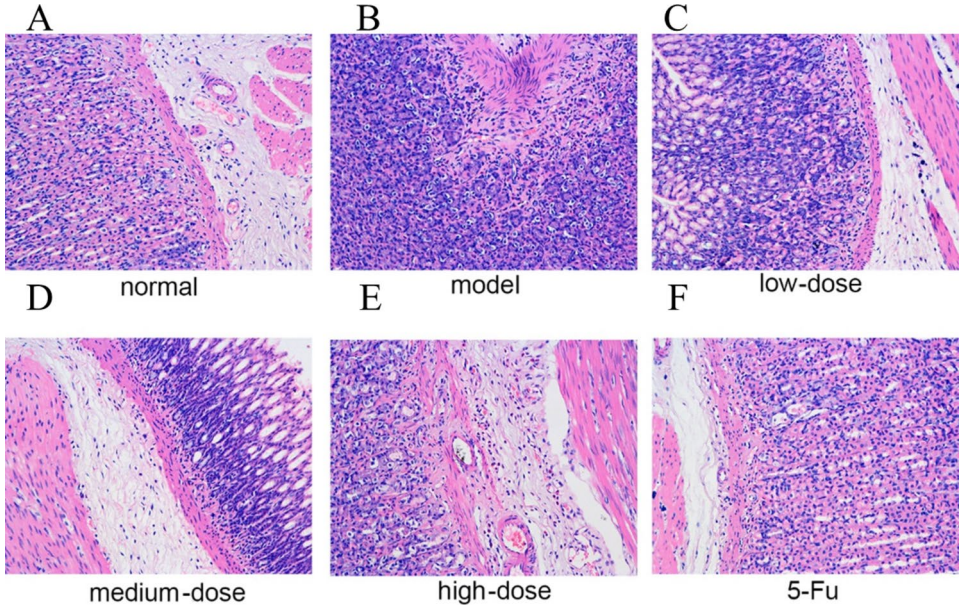

Fig. 2 Sempervirine induces pathological changes in tumor tissues in vivo. Tumor-bearing mice were treated with sempervirine (low-dose1 mg/kg, mediun-dose 3 mg/kg, high-dose10 mg/kg) or vehicle control daily for 2 weeks. Tumor tissues were excised, sectioned, and stained with H&E. Representative images are shown for control (**A**). model (**B**), sempervirine-treated (**C**-**E**) groups and 5-Fu groups

As shown in Fig.S2, control tumor tissue exhibited normal ultrastructural morphology of organelles. In contrast, sempervirine-treated tumors displayed several ultrastructural abnormalities. These included increased collagen deposition around tumor cells, dilation of the endoplasmic reticulum, and mitochondrial swelling with vacuole formation. Mitochondria in sempervirine-treated tissue appeared enlarged and contained electron-lucent vacuoles. These results demonstrate that sempervirine induced abnormal ultrastructural changes in tumor tissues, including alterations to the extracellular matrix, endoplasmic reticulum, and mitochondria. This provides insight into the potential mechanisms by which sempervirine exerts its anticancer effects at the subcellular level. Further studies are required to elucidate the molecular pathways involved in sempervirine's disruption of tumor ultrastructure and organelle integrity.

In summary, compared to the control group, drug administration markedly induced pathological and ultrastructural changes of mouse tumor tissues, manifested as poorly developed tumor mucosa and intracellular structural damage. The high dose administration demonstrated effects close to the positive control drug 5-Fu. This indicates the compound was able to successfully elicit pathological changes of tumor cells.

Effect of sempervirine on SKOV3 colony formation

To evaluate the impact of sempervirine on the colony formation ability of SKOV3 cells, concentrations of 2.5 μM, 5 μM, and 10 μM were selected for treatment. The results showed that the colony formation rate in the solvent control group was 100.00 ± 3.42. In contrast, the colony formation rates for the 2.5 μM, 5 μM, and 10 μM treatment groups were 82.83 ± 3.54, 47.31 ± 1.84, and 35.29 ± 2.31, respectively (Fig. 3A, B). These findings indicate that sempervirine significantly inhibits SKOV3 colony formation in a dose-dependent manner.

Apoptosis analysis

To assess the effect of sempervirine on SKOV3 cell apoptosis, Annexin V-APC/PI staining was performed and apoptosis rates were analyzed by flow cytometry. The results demonstrated that the apoptosis rates in the solvent control, 2.5 μM, 5 μM, and 10 μM treatment groups were 2.67 ± 0.38, 3.49 ± 0.46, 13.01 ± 0.01, and 41.25 ± 0.59, respectively (Fig. 4A, B). These results suggest that sempervirine induces apoptosis in SKOV3 cells in a dose-dependent manner.

Cell cycle analysis

Flow cytometry results revealed the distribution of SKOV3 cells in different phases of the cell cycle after treatment with sempervirine. In the solvent control group, the percentage of cells in the G1 phase was 74.81 ± 0.38, while in the 2.5 μM, 5 μM, and 10 μM treatment groups, the G1 phase cell percentages were 66.68 ± 0.43, 52.05 ± 0.54, and 53.33 ± 0.59, respectively. For the S phase, the cell percentages were 15.48 ± 0.35 in the control group, and 10.37 ± 0.19, 18.61 ± 0.51, and 24.51 ± 0.78 in the 2.5 μM, 5 μM, and 10 μM treatment groups, respectively. Similarly, the G2/M phase cell percentages were 9.70 ± 0.30 for the control group, and 22.95 ± 0.50, 29.39 ± 0.17, and 22.16 ± 0.35 for the 2.5 μM, 5 μM, and 10 μM groups, respectively (Fig. 4 C, D).

RNA-sequencing of SKOV3 cells treatment with sempervirine

To elucidate the biological effects observed in the sempervirine/control group, we conducted transcriptome sequencing for both the sempervirine/control group. Transcriptome sequencing analysis identified a total of 3,872 upregulated genes and 3,153 downregulated genes (Fig. 5A, B). Gene Ontology (GO) enrichment analysis of the differentially expressed genes revealed significant enrichment in biological processes such as regulation of

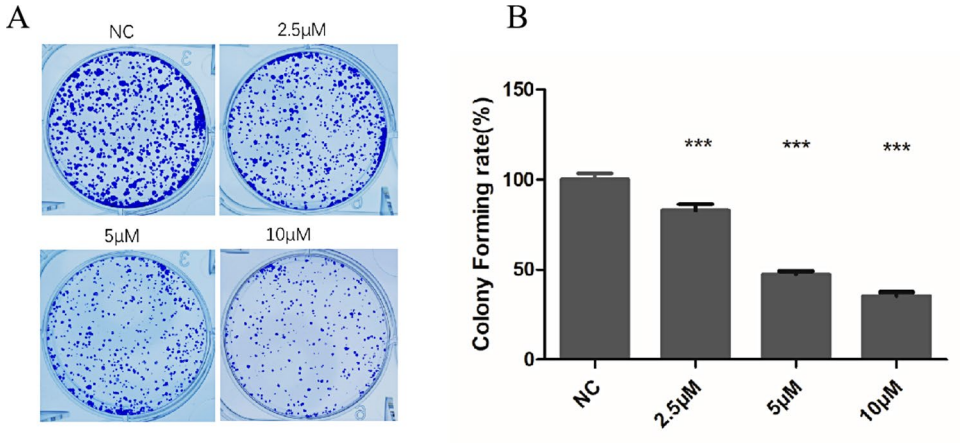

Fig. 3 (**A**) Colony formation assay showing the dose-dependent inhibition of SKOV3 colony formation by sempervirine at concentrations of 2.5 μM, 5 μM, and 10 μM. The colony formation rates are expressed as percentages relative to the solvent control group

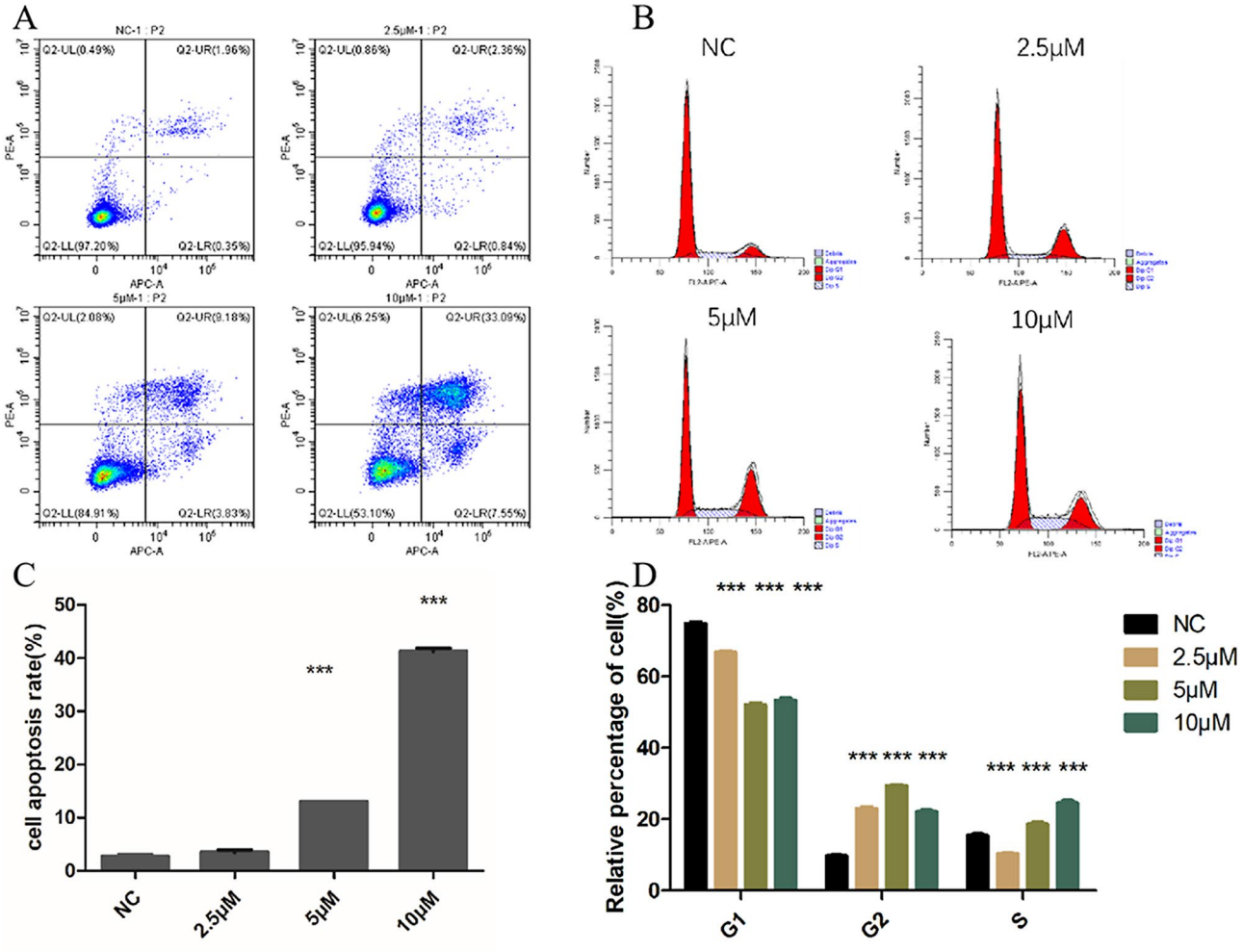

Fig. 4 (**A**, **C**) Flow cytometry analysis of apoptosis using Annexin V-APC/PI staining. The percentage of apoptotic cells significantly increased in a dose-dependent manner, with the highest apoptosis rate observed in the 10 μM sempervirine treatment group; (**B**, **D**) Cell cycle distribution of SKOV3 cells treated with sempervirine. Flow cytometry results indicate a decrease in the G1 phase and an increase in the S and G2/M phases, suggesting cell cycle arrest at these stages. Data are presented as mean ± SD from three independent experiments

transcription, DNA-templated, regulation of transcription by RNA polymerase II, protein phosphorylation, and regulation of PI3K activity (Fig. 5 C). Additionally, KEGG pathway enrichment analysis demonstrated that the differentially expressed genes were significantly enriched in pathways including Mitophagy, Autophagy, MAPK signaling pathway, Apoptosis, and TNF signaling pathway (Fig. 5D).

Sempervirine downregulates apelin signaling pathway

To investigate the molecular mechanisms of sempervirine, we examined its effects on the Apelin signaling pathway, which plays a key role in ovarian carcinogenesis. As presented in Fig. 6, sempervirine remarkably decreased the protein expression of Apelin and CD34 mRNA and protein in ovarian cancer were examined. Since Apelin and CD34 play critical roles in angiogenesis of ovarian cancer, we tested whether the effects of the compound were mediated through blocking Apelin and CD34 expression in ovarian cancer prelesions. As shown in the figure, compound treatment significantly increased the levels of Apelin and CD34 mRNA in the tissues. The compound blocked the elevation of Apelin and CD34 mRNA levels in tumor tissues in a dose-dependent manner (Fig. 6). Consistent with mRNA results, compound treatment also prevented the increase of Apelin and CD34 protein levels in tumor tissues (Fig. 6). Additionally, immunohistochemical staining for Apelin and CD34 was performed. As shown in the Figure S3, compound treatment markedly increased the expression of Apelin and CD34 in the ovarian epithelium, while compound treatment dose-dependently reduced the overexpression of Apelin and CD34 induced by the compound. The inhibitory effects of high-dose compound were comparable to that of the positive control 5-Fu group.

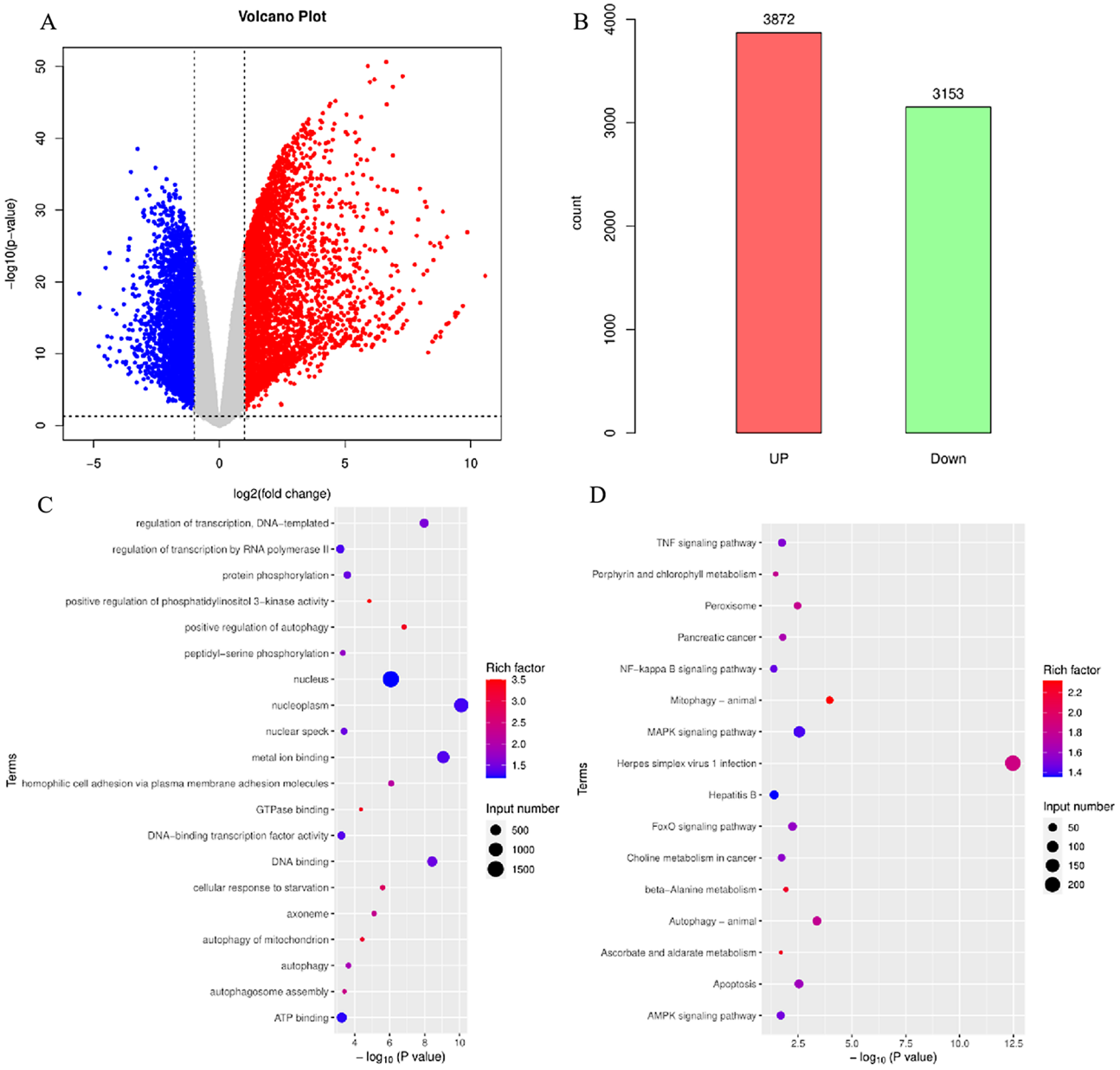

Fig. 5 RNA sequencing revealed a significant upregulation of cellular energy metabolism and synthesis-related pathways in the sempervirine/control group. (**A**) Volcano plot of upregulated and downregulated genes; (**B**) Number of differential gene expression between sempervirine and control groups; with mTOR notably upregulated in the sempervirine/control group. (**C**) Bubble chart of z-score from GO enrichment analysis. (**D**) Bubble chart of z-score from KEGG enrichment analysis

Discussion

Sempervirine, an isoquinoline alkaloid isolated from the traditional Chinese medicine Menispermum dauricum Rhizoma, possesses anti-inflammatory, antipyretic, antioxidant, antimicrobial and anti-tumor properties [20, 23]. Its anti-tumor effects are manifested as inhibition of cancer cell proliferation and induction of apoptosis in various malignancies including breast cancer [24], hepatocellular carcinoma [25], Glioma [26].Besides direct tumor-killing effects, mounting evidence has shown that sempervirine possesses anti-angiogenic property. Tumor growth, progression and metastasis rely on sufficient nutrition and oxygen supply, which is supported by angiogenesis [27].

Sempervirine is a bioactive compound with significant anticancer potential, exerting its effects through the modulation of key cellular pathways. It induces cell cycle arrest, particularly at the G1 phase, preventing cancer cells from progressing to the DNA synthesis (S) phase and thereby inhibiting proliferation [25]. Notably, sempervirine is effective in both p53 wild-type and p53-mutant or deficient cancer cells [20], making it broadly

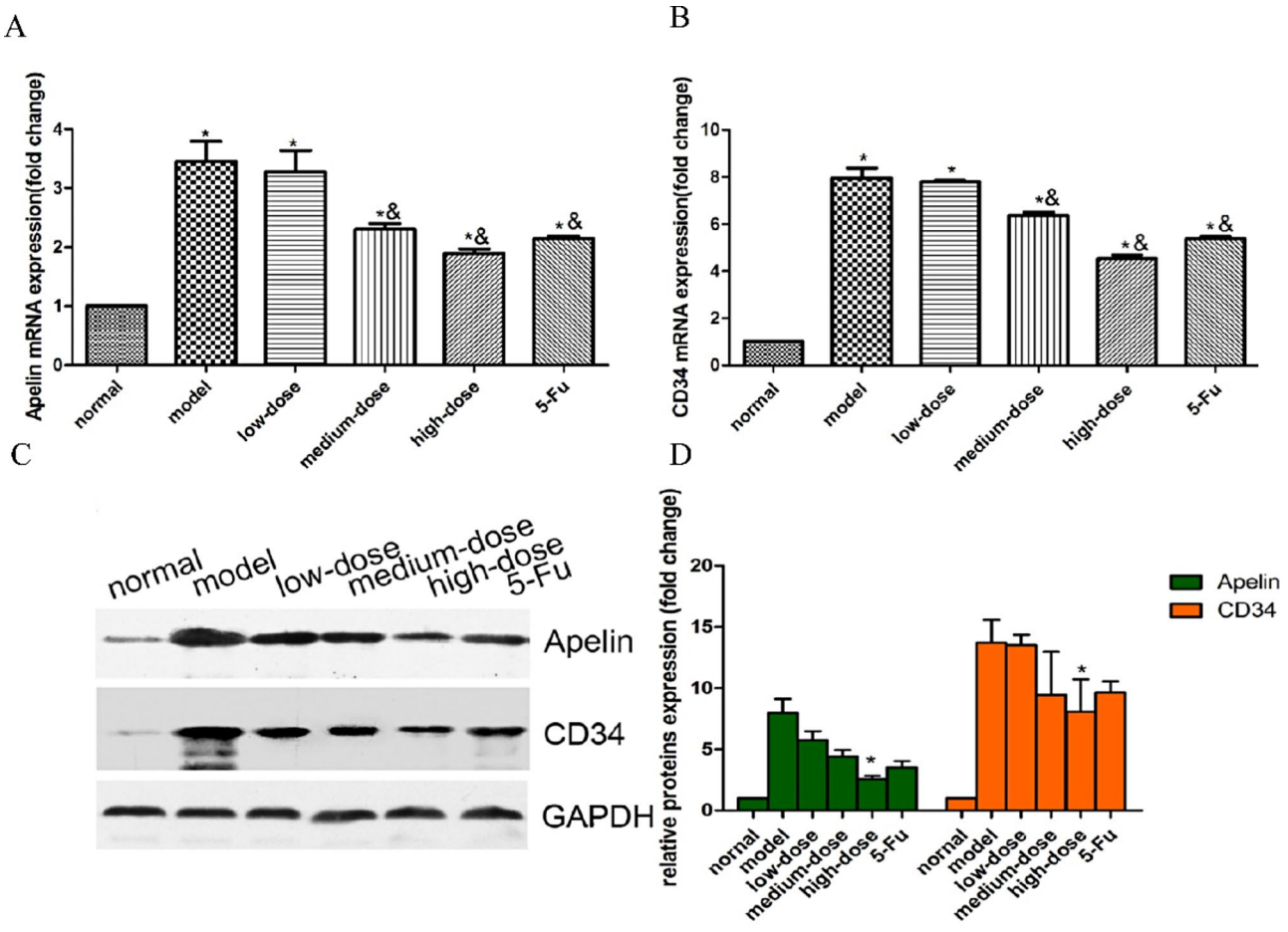

Fig. 6 Sempervirine significantly decreased apelin and CD34. (**A**) qPCR analysis showed sempervirine significantly decreased apelin and CD34 mRNA levels in a dose-dependent manner in SKOV3 cells. (**B**) In tumor tissues, sempervirine dose-dependently blocked elevated expression of apelin and CD34 mRNA compared to control. (**C**) Western blot analysis demonstrated increased apelin and CD34 protein expression in SKOV3 cells following sempervirine treatment. (**D**) Similarly, sempervirine dose-dependently prevented increased apelin and CD34 protein levels in tumor tissues. The inhibitory effect of high dose sempervirine was comparable to positive control 5-Fu

applicable in various tumor types. It also modulates critical signaling pathways such as Wnt/β-catenin [25] and Akt/mTOR [26], both of which play essential roles in cancer progression. By inhibiting the Wnt/β-catenin pathway, Sempervirine reduces cancer cell proliferation, while its inhibition of the Akt/mTOR pathway leads to autophagy and apoptosis induction. Furthermore, sempervirine promotes apoptosis through the cleavage of caspase-3, a key apoptotic marker. Although research specifically on ovarian cancer is limited, the demonstrated efficacy of Sempervirine in other cancers suggests its potential as a novel therapeutic option for ovarian cancer, particularly in overcoming resistance to conventional therapies.

Natural products have long been valuable sources of novel therapeutic agents for cancer treatment. Over the past decades, many anticancer drugs have been developed from active components identified in medicinal plants, such as paclitaxel, camptothecin and vinblastine [11]. Bulbus Fritillaria herbs contain diverse alkaloids with extensive pharmacological activities and have been clinically used for treating different types of cancers [12]. Uncontrolled proliferation is a hallmark of cancer cells [28]. Tumor metastasis accounts for over 90% of ovarian cancer-related deaths but remains the most poorly understood aspect of ovarian cancer pathogenesis [29]. We found that sempervirine significantly inhibited the invasive capacities of ovarian cancer cells. Cancer metastasis is a complex multistep process that requires cancer cells to detach from primary sites, migrate, invade into circulation, and proliferate at distant sites [30].

In vivo studies further validated the antitumor efficacy of sempervirine in subcutaneous and orthotopic ovarian cancer xenograft models. Sempervirine dramatically suppressed tumor growth by inhibiting cell proliferation and inducing apoptosis. Ultrastructural analysis by transmission electron microscopy revealed that sempervirine induced damage of tumor cell structures. Moreover, sempervirine displayed minimal toxicity in mice as evidenced

by unchanged body weight. These results highlight the translational potential of sempervirine for ovarian cancer treatment.

Mechanistic studies found that sempervirine could downregulate the expression of several key proteins involved in the Apelin signaling pathway. Aberrant activation of Apelin signaling has been associated with ovarian carcinogenesis and progression [31]. Targeting Apelin pathway has become a promising treatment strategy for ovarian cancer [32]. Therefore, inhibition of Apelin signaling may confer the anticancer activities of sempervirine against ovarian cancer. Further investigations on the precise molecular mechanisms are required to fully elucidate the antitumor effects of sempervirine.

The growth factor apelin and surface marker CD34 play critical roles in ovarian cancer angiogenesis [33, 34]. Apelin can directly act on vascular endothelial cells in ovarian tumor microenvironment and promote their proliferation, migration and tube formation [35]. Apelin also upregulates expression of pro-angiogenic factors like VEGF, synergistically facilitating tumor angiogenesis with endothelial cells [36]. CD34 is a characteristic pan-endothelial marker [37]. In summary, apelin and CD34 are important contributors to ovarian cancer angiogenesis. As a natural isoquinoline alkaloid that can inhibit ovarian cancer angiogenesis, and based on its ability to decrease expression of key pro-angiogenic factors such as VEGF, we hypothesize sempervirine may also exert anti-angiogenic and anti-tumor effects by suppressing apelin and CD34 expression and functions.

The occurrence and development of ovarian cancer is closely related to tumor angiogenesis. Apelin is a widely expressed growth factor that can bind to its specific receptor APJ and activate multiple downstream signaling pathways involved in the regulation of angiogenesis [38]. In various tumors, including ovarian cancer, high expression of Apelin is associated with tumor angiogenesis and progression [35]. Specifically in ovarian cancer, Apelin can directly act on vascular endothelial cells to promote their proliferation, migration, and tube formation, thereby stimulating tumor angiogenesis. In addition, Apelin can upregulate expression of ovarian cancer cell-intrinsic angiogenic markers such as VEGF to exert a dual pro-angiogenic effect. CD34 is a pan-endothelial cell marker and also marks mesenchymal stem cells and hematopoietic stem cells [37].

In this study, we demonstrated for the first time that sempervirine, an alkaloid isolated from traditional Chinese medicine Bulbus Fritillaria, possesses potent anti-ovarian cancer activities both in vitro and in vivo. Sempervirine significantly inhibited ovarian cancer cell proliferation, invasion and tumor growth. Mechanistic studies revealed that the anticancer effects of sempervirine were mediated through downregulation of Apelin signaling pathway. Nonetheless, there are still limitations in the current study. Although the in vivo xenograft models showed promising antitumor effects of sempervirine, mouse models cannot fully recapitulate the complexity of human ovarian cancer. Testing sempervirine using patient-derived xenograft (PDX) models that better represent tumor heterogeneity will provide more clinically relevant evidence. Moreover, while we revealed the involvement of Apelin signaling, the precise mechanisms of action of sempervirine remain to be fully defined. Global approaches such as transcriptomics and proteomics could help identify its direct molecular targets. Additionally, exploring the effects of sempervirine on tumor microenvironment crosstalk and antitumor immunity using syngeneic mouse models will provide further insights into its therapeutic mechanisms. Finally, pharmacokinetic and toxicological evaluation, as well as pharmaceutical optimization and delivery strategies for sempervirine are needed to facilitate its clinical translation.

Conclusion

In conclusion, our study demonstrates for the first time that sempervirine, a natural alkaloid derived from traditional Chinese medicine, possesses significant anti-ovarian cancer activities. We have shown that sempervirine can effectively inhibit ovarian cancer cell proliferation, invasion and tumor growth through downregulating Apelin signaling. These profound antitumor effects were validated both in vitro and in vivo using ovarian cancer cell lines and xenograft mouse models. Our findings provide strong preclinical evidence supporting sempervirine as a promising natural agent for ovarian cancer treatment. Further investigations to elucidate its precise molecular mechanisms of action, pharmacokinetic properties, toxicity profiles and pharmaceutical preparations are warranted to promote the clinical translation of sempervirine as a novel therapeutic for ovarian cancer. In summary, sempervirine represents a potential effective anticancer drug candidate which merits further development through preclinical and clinical studies for the ultimate benefit of ovarian cancer patients.

Supplementary Information

The online version contains supplementary material available at https://doi.org/10.1186/s13048-024-01580-4.

Supplementary Material 1

Author contributions

Danni Chen, Yan Tan and Tingting Chen wrote the main manuscript text and Qin Wang, Yan Yan and Xiaoya Zhao prepared figures . Zhongxiao Zhang was responsible for the animal experiment.Jin Qiu and Jian Zhang were responsible fordesigning the research project and revising the manuscript.All authors reviewed the manuscript.

Funding
This work was supported by a grant from the Science and Technology Commission of Changning District, Shanghai (Grant No CNKW2022Y16 to D.C), and a grant from the Health Commission of Changning District, Shanghai(Grant No RCJD2021S01 to J.Q).

Data availability
No datasets were generated or analysed during the current study.

Declarations

Competing interests
The authors declare no competing interests.

Received: 6 July 2024 / Accepted: 11 December 2024
Published online: 28 January 2025

References

1. Erratum. Global cancer statistics 2018: GLOBOCAN estimates of incidence and mortality worldwide for 36 cancers in 185 countries. CA Cancer J Clin. 2020;70(4):313.
2. Penny SM. Ovarian Cancer: an overview. Radiol Technol. 2020;91(6):561–75.
3. Stewart C, Ralyea C, Lockwood S. Ovarian Cancer: an Integrated Review. Semin Oncol Nurs. 2019;35(2):151–6.
4. Coleman RL, Monk BJ, Sood AK, Herzog TJ. Latest research and treatment of advanced-stage epithelial ovarian cancer. Nat Rev Clin Oncol. 2013;10(4):211–24.
5. Morand S, Devanaboyina M, Staats H, Stanbery L, Nemunaitis J. Ovarian Cancer Immunotherapy and Personalized Medicine. Int J Mol Sci 2021, *22* (12).
6. Vaughan S, Coward JI, Bast RC Jr., Berchuck A, Berek JS, Brenton JD, Coukos G, Crum CC, Drapkin R, Etemadmoghadam D, Friedlander M, Gabra H, Kaye SB, Lord CJ, Lengyel E, Levine DA, McNeish IA, Menon U, Mills GB, Nephew KP, Oza AM, Sood AK, Stronach EA, Walczak H, Bowtell DD, Balkwill F. R., Rethinking ovarian cancer: recommendations for improving outcomes. Nat Rev Cancer. 2011;11(10):719–25.
7. Galluzzi L, Senovilla L, Vitale I, Michels J, Martins I, Kepp O, Castedo M, Kroemer G. Molecular mechanisms of cisplatin resistance. Oncogene. 2012;31(15):1869–83.
8. Han L, Chen Y, Zheng A, Chen H. Incidence and risk factors for venous thromboembolism in patients with ovarian cancer during neoadjuvant chemotherapy: a meta-analysis. Am J Cancer Res. 2023;13(5):2126–34.
9. Gordaliza M. Natural products as leads to anticancer drugs. Clin Transl Oncol. 2007;9(12):767–76.
10. Newman DJ, Cragg GM. Natural products as sources of New drugs over the nearly four decades from 01/1981 to 09/2019. J Nat Prod. 2020;83(3):770–803.
11. Buyel JF. Plants as sources of natural and recombinant anti-cancer agents. Biotechnol Adv. 2018;36(2):506–20.
12. Wang L, Jiang Y, Yaseen A, Li F, Chen B, Shen XF, Zheng C, Zhang GL, Wang MK. Steroidal alkaloids from the bulbs of Fritillaria Pallidiflora Schrenk and their anti-inflammatory activity. Bioorg Chem. 2021;112:104845.
13. Jin GL, Su YP, Liu M, Xu Y, Yang J, Liao KJ, Yu CX. Medicinal plants of the genus Gelsemium (Gelsemiaceae, Gentianales)--a review of their phytochemistry, pharmacology, toxicology and traditional use. J Ethnopharmacol. 2014;152(1):33–52.
14. Cao EC, o. ZHB. Zhong Hua Ben Cao. Shanghai: Shanghai Scientific and Technical Publishers China; 1999.
15. Bentley R, Stevens TS. Structure of sempervirine. Nature. 1949;164(4160):141.
16. Pan X, Yang C, Cleveland JL, Bannister TD. Synthesis and cytoxicity of Sempervirine and Analogues. J Org Chem. 2016;81(5):2194–200.
17. Sucunza D, Cuadro AM, Alvarez-Builla J, Vaquero JJ. Recent advances in the synthesis of Azonia Aromatic Heterocycles. J Org Chem. 2016;81(21):10126–35.
18. Kerkovius JK, Kerr MA. Total synthesis of Isodihydrokoumine, (19 Z)-Taberpsychine, and (4 R)-Isodihydroukoumine N(4)-Oxide. J Am Chem Soc. 2018;140(27):8415–9.
19. Beljanski M, Beljanski MS. Three alkaloids as selective destroyers of cancer cells in mice. Synergy with classic anticancer drugs. Oncology. 1986;43(3):198–203.
20. Caggiano C, Guida E, Todaro F, Bielli P, Mori M, Ghirga F, Quaglio D, Botta B, Moretti F, Grimaldi P, Rossi P, Jannini EA, Barchi M, Dolci S. Sempervirine inhibits RNA polymerase I transcription independently from p53 in tumor cells. Cell Death Discov. 2020;6(1):111.
21. Fulda S, Scaffidi C, Pietsch T, Krammer PH, Peter ME, Debatin KM. Activation of the CD95 (APO-1/Fas) pathway in drug- and gamma-irradiation-induced apoptosis of brain tumor cells. Cell Death Differ. 1998;5(10):884–93.
22. Lin L, Hutzen B, Lee HF, Peng Z, Wang W, Zhao C, Lin HJ, Sun D, Li PK, Li C, Korkaya H, Wicha MS, Lin J. Evaluation of STAT3 signaling in ALDH + and ALDH+/CD44+/CD24- subpopulations of breast cancer cells. PLoS ONE 2013, 8 (12), e82821.
23. Deng B, Jiang XL, Tan ZB, Cai M, Deng SH, Ding WJ, Xu YC, Wu YT, Zhang SW, Chen RX, Kan J, Zhang EX, Liu B, Zhang JZ. Dauricine inhibits proliferation and promotes death of melanoma cells via inhibition of Src/STAT3 signaling. Phytother Res. 2021;35(7):3836–47.
24. Avtanski DB, Nagalingam A, Tomaszewski JE, Risbood P, Difillippantonio MJ, Saxena NK, Malhotra SV, Sharma D. Indolo-pyrido-isoquinolin based alkaloid inhibits growth, invasion and migration of breast cancer cells via activation of p53-miR34a axis. Mol Oncol. 2016;10(7):1118–32.
25. Yue R, Liu H, Huang Y, Wang J, Shi D, Su Y, Luo Y, Cai P, Jin G, Yu C. Sempervirine inhibits proliferation and promotes apoptosis by regulating Wnt/β-Catenin pathway in human hepatocellular carcinoma. Front Pharmacol. 2021;12:806091.
26. Li G, Zhong Y, Wang W, Jia X, Zhu H, Jiang W, Song Y, Xu W, Wu S. Sempervirine mediates autophagy and apoptosis via the Akt/mTOR signaling pathways in Glioma cells. Front Pharmacol. 2021;12:770667.
27. Hanahan D, Folkman J. Patterns and emerging mechanisms of the angiogenic switch during tumorigenesis. Cell. 1996;86(3):353–64.
28. Hanahan D, Weinberg RA. Hallmarks of cancer: the next generation. Cell. 2011;144(5):646–74.
29. Lengyel E. Ovarian cancer development and metastasis. Am J Pathol. 2010;177(3):1053–64.
30. Valastyan S, Weinberg RA. Tumor metastasis: molecular insights and evolving paradigms. Cell. 2011;147(2):275–92.
31. Altomare DA, Wang HQ, Skele KL, De Rienzo A, Klein-Szanto AJ, Godwin AK, Testa JR. AKT and mTOR phosphorylation is frequently detected in ovarian cancer and can be targeted to disrupt ovarian tumor cell growth. Oncogene. 2004;23(34):5853–7.
32. Mabuchi S, Altomare DA, Cheung M, Zhang L, Poulikakos PI, Hensley HH, Schilder RJ, Ozols RF, Testa JR. RAD001 inhibits human ovarian cancer cell proliferation, enhances cisplatin-induced apoptosis, and prolongs survival in an ovarian cancer model. Clin Cancer Res. 2007;13(14):4261–70.
33. Masoumi J, Jafarzadeh A, Khorramdelazad H, Abbasloui M, Abdolalizadeh J, Jamali N. Role of Apelin/APJ axis in cancer development and progression. Adv Med Sci. 2020;65(1):202–13.
34. Błochowiak KJ, Sokalski J, Bodnar MB, Trzybulska D, Marszałek AK, Witmanowski H. Expression of $VEGF_{165}b$, VEGFR1, VEGFR2 and CD34 in benign and malignant tumors of parotid glands. Adv Clin Exp Med. 2018;27(1):83–90.
35. Sorli SC, Le Gonidec S, Knibiehler B, Audigier Y. Apelin is a potent activator of tumour neoangiogenesis. Oncogene. 2007;26(55):7692–9.
36. Cox CM, D'Agostino SL, Miller MK, Heimark RL, Krieg PA. Apelin, the ligand for the endothelial G-protein-coupled receptor, APJ, is a potent angiogenic factor required for normal vascular development of the frog embryo. Dev Biol. 2006;296(1):177–89.
37. Sidney LE, Branch MJ, Dunphy SE, Dua HS, Hopkinson A. Concise review: evidence for CD34 as a common marker for diverse progenitors. Stem Cells. 2014;32(6):1380–9.
38. Sorli SC, van den Berghe L, Masri B, Knibiehler B, Audigier Y. Therapeutic potential of interfering with apelin signalling. Drug Discov Today. 2006;11(23–24):1100–6.

Publisher's note